Supplementary Material

Figure S1. **Time evolution of the root-mean-square (RMS) deviation in Glt_{ph} atomic coordinates.** The RMS deviations refer to the departure from the original (X-ray) coordinates averaged over all atoms, observed in three runs: MD0 (panel ***A***), MD5 (panel ***B***) and MD6 (panel ***C***). See Table 1 for the descriptions of the runs. Black, green and red curves refer to the results for the respective subunits A, B and C of the homotrimer. The RMS deviation profiles exhibit a sharp increase to about 2 Å within the first equilibration period of 0.2 ns, and remain lower than 4.0 Å throughout the succeeding 40 ns MD0 simulations. Relatively larger deviations are observed in the presence of higher concentrations of ligand and ions (panels B and C).

Figure S2. **RMS fluctuation in residue positions observed in the first 10 ns portion of the run MD0**. The RMS fluctuations refer to the departures from mean positions of individual residues (C^{α}-atoms), observed during the simulations. The three curves describe the profiles for subunits A (black), B (red) and C (green). The secondary structural elements are indicated by horizontal bars along the upper abscissa. The loop L34 between helices TM3 and TM4 exhibits large fluctuations in all three subunits. Subunit A is distinguished by a large motion at the hairpin HP2.

Figure S3. **Interhelical interactions that control the gating motions of the HP2 loop.** Two pairs of interhelical contacts, between G351 (HP2 tip) and I309 (TM7), and between A345 (HP2a) and Q318 (TM7) were observed to restrict the mobility of HP2, preventing this putative EC gate from complete opening or destabilization. The positions of these residues in the core domain are shown on the ribbon diagram, and the time profile of three particular contacts that involve Q318 is displayed on the left panel. We note that the contact between Q318-A345 is closely maintained at all times during the 40 ns MD0 run. Looser but stable interactions are also observed between Q318 and A348 on the adjoining helical turn, whereas the interaction with G359 is weaker but effective as a back up mechanism.

Figure S4. **Mode dispersion derived from essential dynamics analysis of four trajectories.** The six curves in each panel are the eigenvalues corresponding to first eight lowest frequency modes obtained by eigenvalue decomposition of the covariance matrix for the hairpin loops, HP1 and HP2, of the three subunits, taken separately. Comparison of MD0 and MD6 shows that the higher concentration of ions in the bulk (MD6) enhances the mobility of the open subunit EC gate (HP2 of subunit A; black) and this effect is most pronounced in the first two modes. Comparison of MD0 and MD2, on the other hand, shows that substrate binding (MD2) suppresses the mobility of the same HP2 loop in substrate-bound form (HP2A, black). Finally, comparison of MD2 with MD4, shows that Na+ binding (MD4) have a dramatic effect on the motion of the EC gate. Note that the average square displacement of EC gate (HP2A) in mode 1 reduces from 4.4 $(nm)^2$ in MD6, to 2.0, 1.25 and 0.4 $(nm)^2$ in the respective runs MD2, MD0 and MD4.

Figure S5. **Comparison of bound conformation of aspartate from simulations (*left*) and experiments (*right*).** The left panel displays the coordination geometry obtained in our simulations starting from initial conformation of MD0 where the substrate has been placed at the putative binding site, and allowed to locate its optimal conformation by an energy minimization followed by a productive run of 2 ns. The right panel displays the structure resolved by Boudker et al (7). The two structures exhibit striking similarities, lending support to the validity of MD simulations.

Figure S6. **Mediation of glutamate binding by water molecules**. Six snapshots from MD1 time interval $0 \leq t \leq 4$ ns are shown to illustrate the movements of five water molecules originally dispersed at various locations in the EC region. The first water molecule enters through the opening between HP2 and HP1 to bind T314 on TM7 (see Supplementary Material, *Figs.S2* and *S3* and ***Movies 2*** and ***3***). Strikingly, this molecule remains at that position even after the glutamate binds (around 1 ns) and locks the entry/exit pathway. The remaining four water molecules are positioned to orderly enter the binding site through another interstice after 2.5 ns (snapshot at 3.55 ns), attracted by D390 and D394 on TM8. Successive entry

of all water molecules takes place in an orderly fashion through the same pathway within 0.3 ns, resulting in the tight interaction between substrate and water molecules in the binding site, on which the HP2 closes down. The glutamate remains tightly bound in the subsequent 6 ns simulations (not shown), while the binding site is solvated at all times by a continuous circulation of water molecules.

Figure S7. **Exchange of water molecule at T314.** The constant presence of a water molecule at T314 on TM7. The four curves (black, green, red and blue) indicate the distance of four different water molecules from the closest atom on T314. The site near T314 is thus occupied by a water molecule at all times.

Figure S8. **High stability of the sodium ion near the substrate binding site and its coordination geometry.** The results here refer to MD3 (Table 1). The Na^+ ion is observed to move down, towards the interior of the core within the first few picoseconds and remains tightly bound at a well-defined position for 10 ns after which the run was discontinued (panel A). We note that the bound Na^+ closely interacts with N310 and D312, two residues that take part in the NMDGT motif on TM7 (panel B). Other residues within 3.5 Å atom-atom interaction range are G306 on TM7 and G404 on TM8.

Figure S9. **Putative binding sites for two Na^+ ions.** The ribbon diagrams on the left show our results from simulations (MD4). The region near the bound sodium ions is magnified, and a few amino acids directly interacting with these ions are explicitly shown. The diagrams on the right are taken from the recent work of Gouaux and coworkers (Boudker et al., 2007) and display the putative Na^+ and aspartate binding sites and the possible mechanism of gate opening proposed in their study. The Na^+ ions are represented as blue spheres (Na1 and Na2), bound glutamate in green, and the water molecules at the binding site as red and white spheres. Note that the first Na^+ near the glutamate is hidden behind the water molecule on the left diagram.

Movie 1: Opening up of the putative extracellular binding site during run MD0. While simulations were performed for the entire trimeric structure in the presence of explicit lipid and water molecules, only the core region of the subunit A is shown here, in which the HP2 loop at the end of the HP2 hairpin (red) moves away from the remaining structural elements of the core domain (HP1 shown in yellow, and the two transmembrane helices TM7 (orange) and TM8 (violet). The secondary structures are colored as per Fi. 1. The total duration of this run is 15ns. (**movie1.md0_core1.avi**)

Movie 2: Diffusion and entry of the glutamate molecule into the binding site in MD1. Only the core of the subunit towards which the glutamate diffuses is shown for clarity. The glutamate is originally attracted by the exposed HP2 loop residues (G354-G357), and then interacts with HP1 (three serine motif), succeeded by TM7 residues D312-T314 and TM8 D394, R397-T398 and D390 that stabilize the bound form (see Fig. 6). The secondary structures are colored as per Figure 1. We also highlight one water molecule (shown in green), which also enters the binding site and remains tightly bound to the residue T314 (see Figure 8). The duration of the trajectory shown is 4 ns **(movie2.md1_core1_glu.avi)**

Movie 3: Diffusion of water molecules into the binding site, in a substrate bound subunit in MD1. Only the core domain of the subunit towards which the water (cyan) and glutamate diffuse are shown, for clarity. The hairpins and helices are colored as in Figure 1. One of the water molecules is shown in green, which binds T314 (see movie 2) and remains bound there for the remainder of the trajectory (total duration 4ns). See also Figure 6. **(movie3.md1_core1_h2o.avi)**

Movie 4: Glutamate and three Na^+ ions in binding site in substrate bound subunit in MD4. Only the core of the subunit of the glutamate bound subunit is shown, for clarity. The hairpin helices are colored as in Figure 1, the Na^+ ions in blue. Two water molecules in the core are highlighted in space-filling representation. The residue interacting with water molecule (T314) and with the $Na^+(1)$ ions (L303 and D405) are indicated in stick representation. One Na^+ ion exits fairly early on during the simulation, while

the two remaing Na^+ ions remain tightly bound to their respective putative binding. These two sites show remarkable agreement with the structural results reported by Boudker et al (2007). **(movie4.md2_core_na_h2o.avi)**

Supplementary Figures

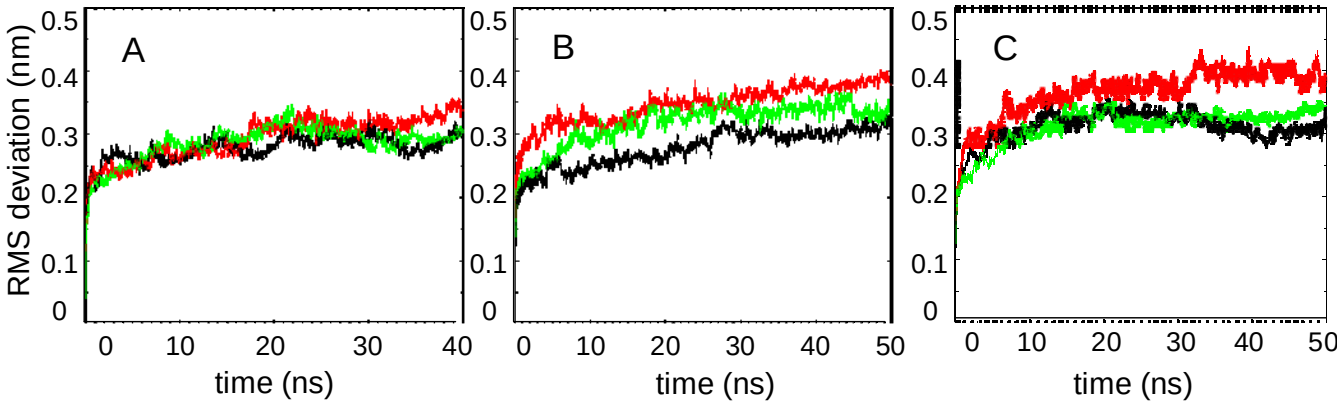

Figure S1

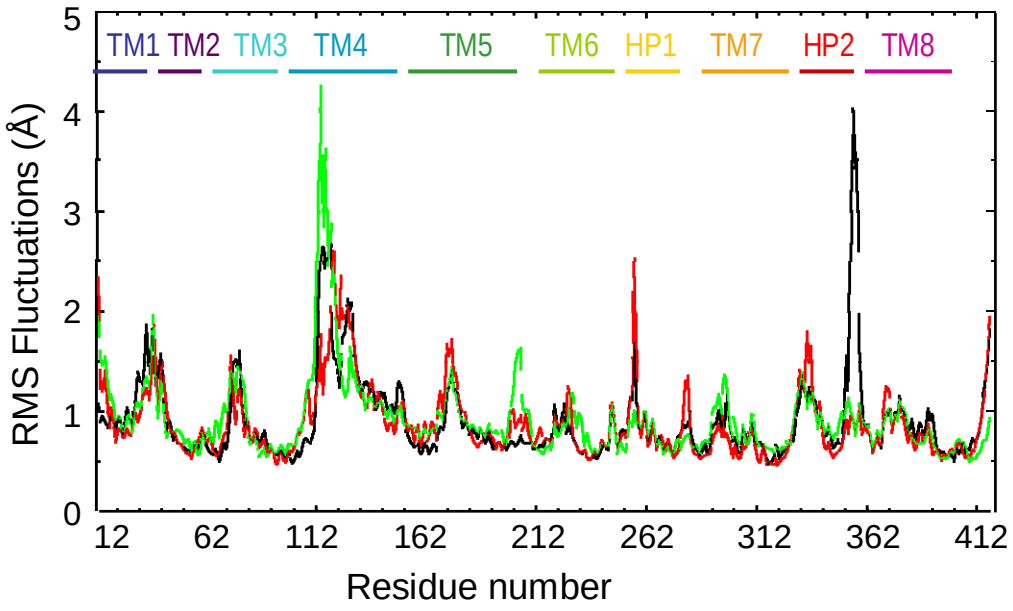
TM1
TM2
TM3
TM4
TM5
TM6
HP1
TM7
HP2
TM8
RMS Fluctuations (Å)
0
1
2
3
4
5
12
62
112
162
212
262
312
362
412
Residue number

Figure S2

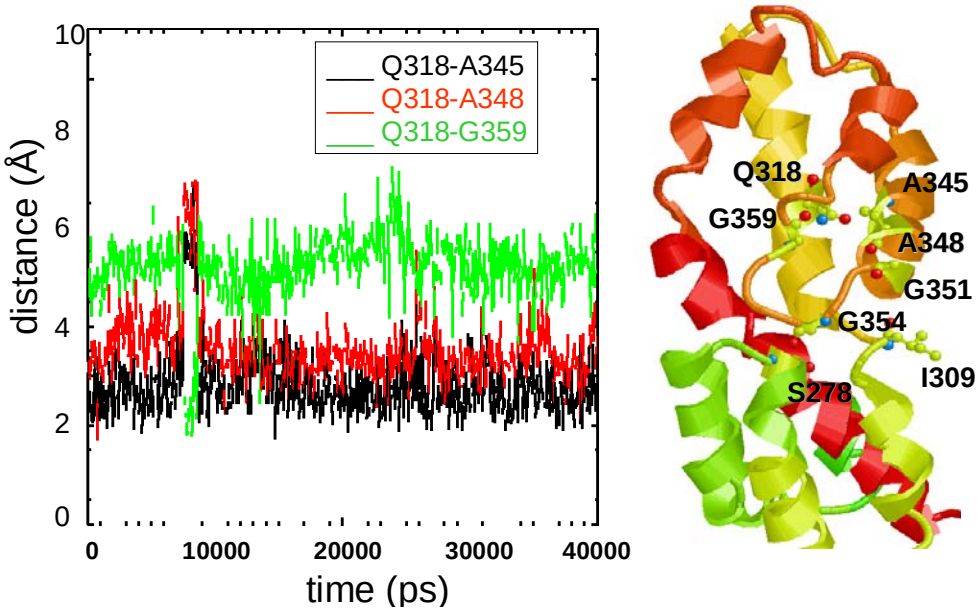
Q318-A345
Q318-A348
Q318-G359
distance (Å)
time (ps)
0
2
4
6
8
10
0
10000
20000
30000
40000
Q318
A345
G359
A348
G351
G354
I309
S278

FigureS3

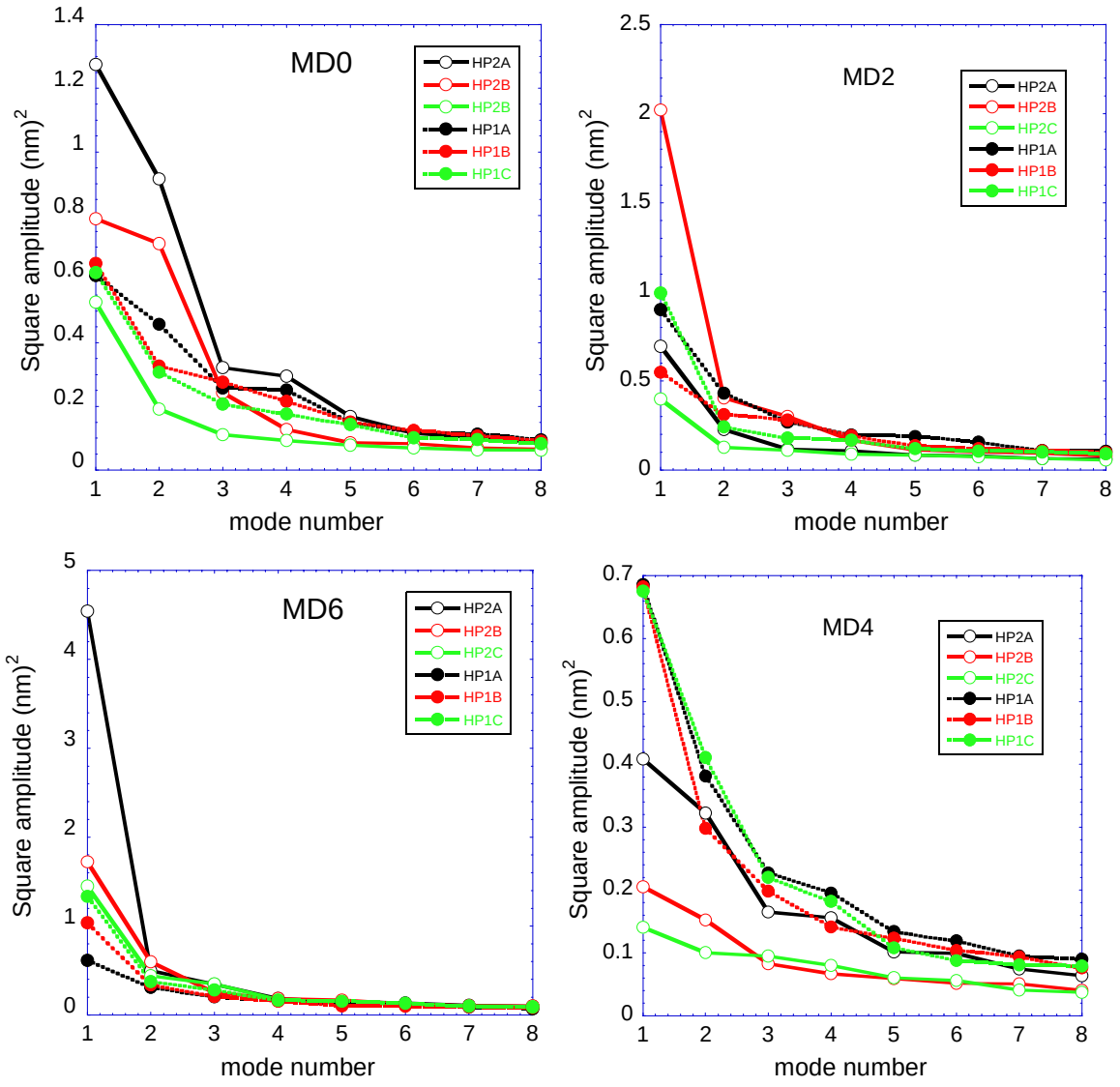
MD0
MD2
MD6
MD4
HP2A
HP2B
HP2B
HP2C
HP1A
HP1B
HP1C
Square amplitude (nm)^2
mode number

Figure S4

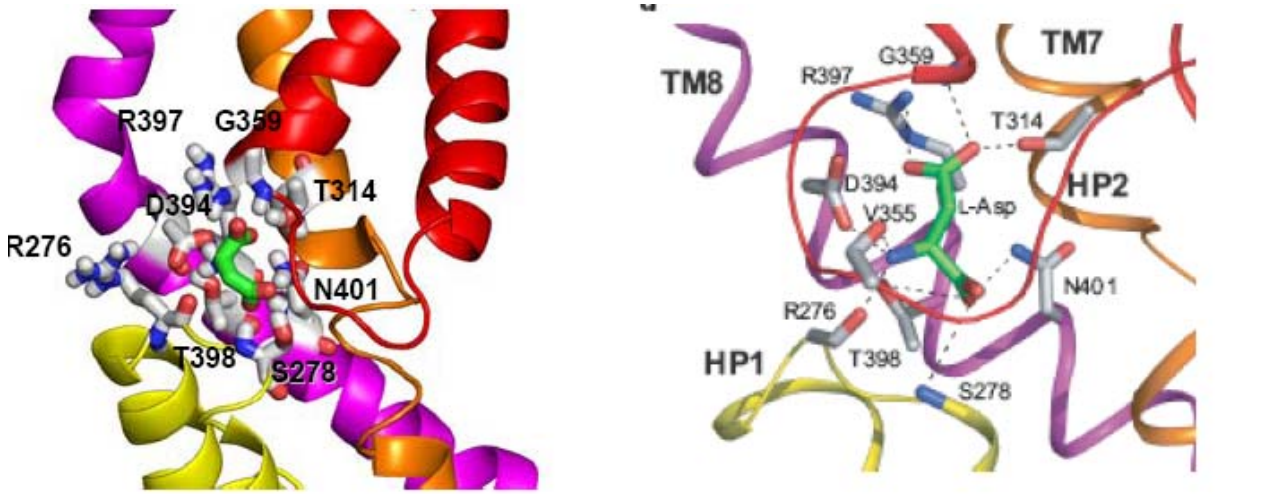

MD simulation snapshot (2ns)

X-ray structure (Boudker et al, *Nature* 2007)

Figure S5

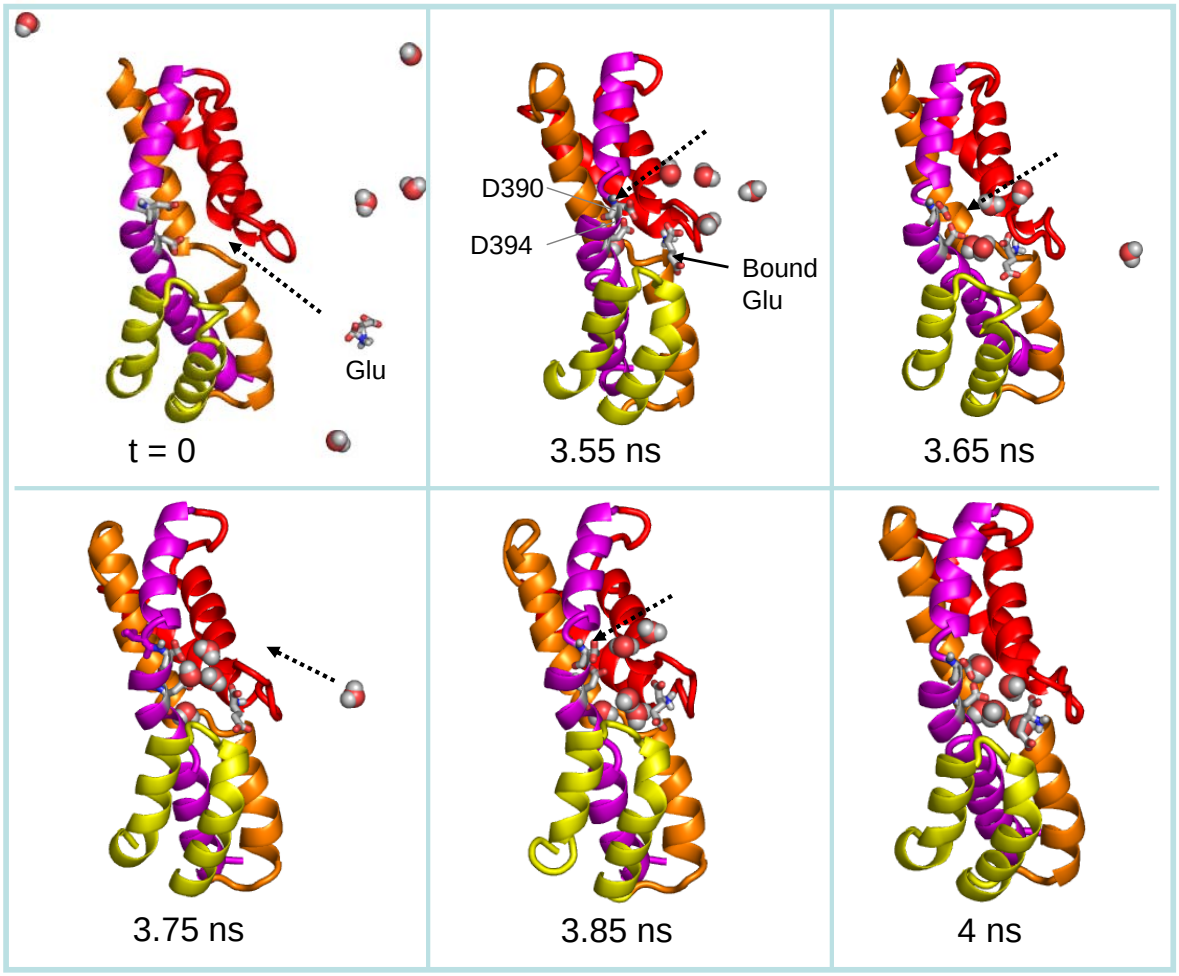

Figure S6

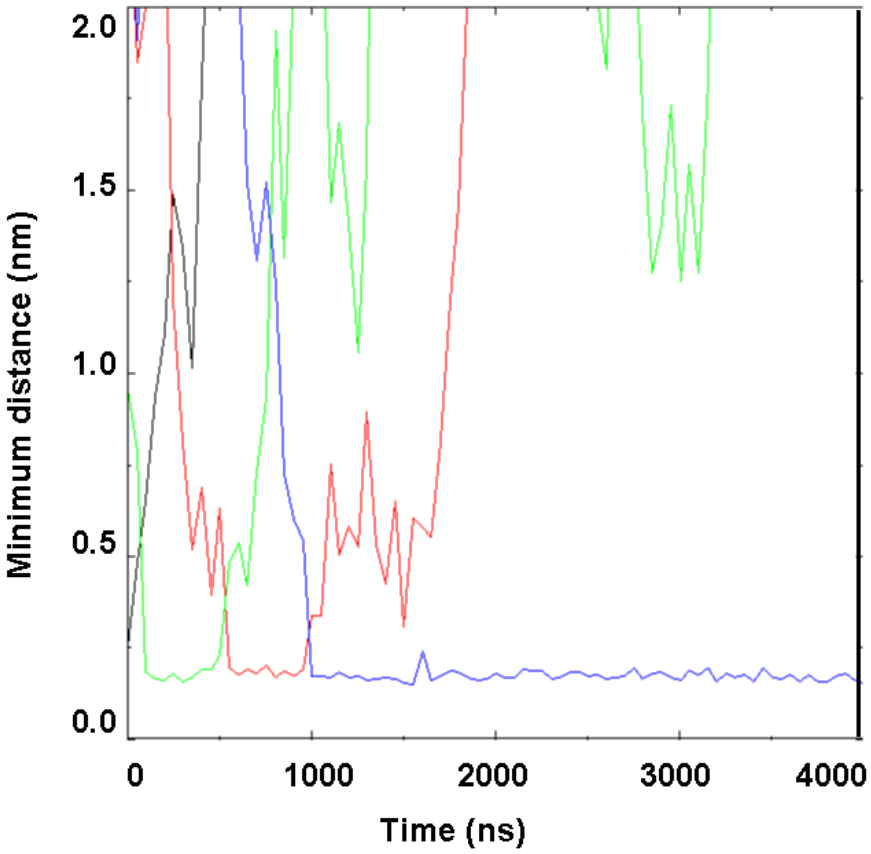
Minimum distance (nm)
2.0
1.5
1.0
0.5
0.0
0
1000
2000
3000
4000
Time (ns)

Figure S7

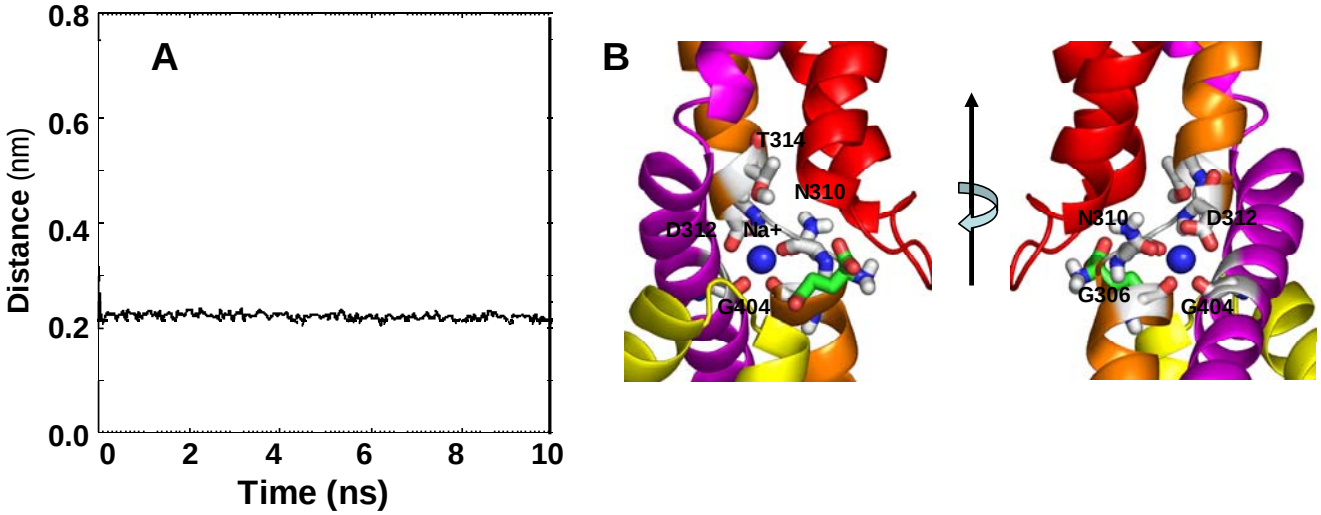
A
Distance (nm)
0.0
0.2
0.4
0.6
0.8
0
2
4
6
8
10
Time (ns)
B
T314
N310
D312
Na+
G404
N310
D312
G306
G404

Figure S8

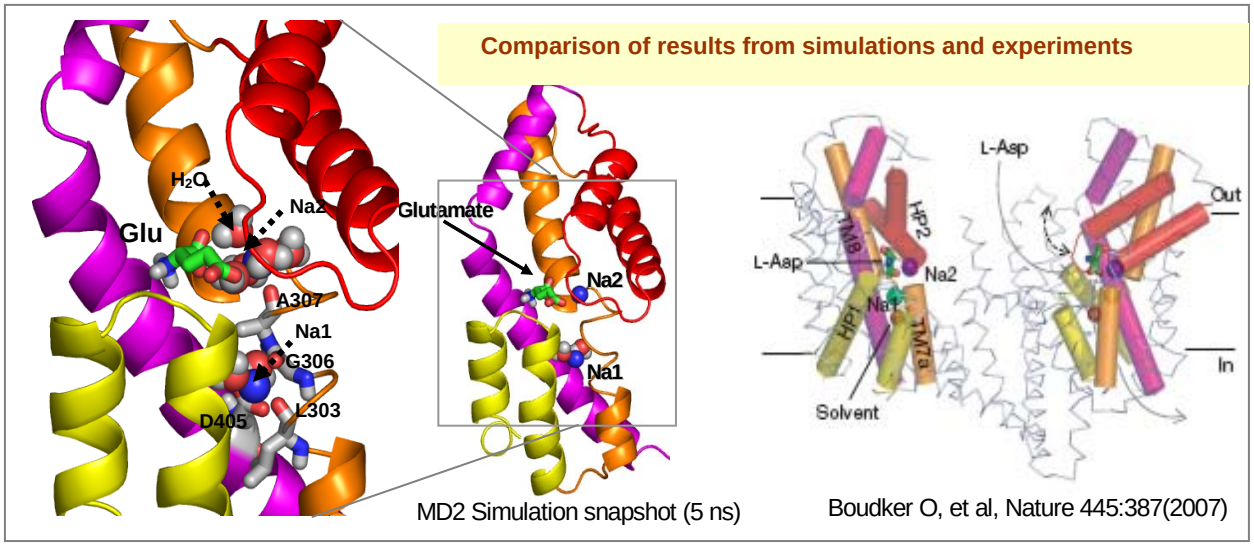
Comparison of results from simulations and experiments
H2O
Na2
Glu
A307
Na1
G306
D405
L303
Glutamate
Na2
Na1
MD2 Simulation snapshot (5 ns)
L-Asp
Out
TM8
HP2
L-Asp
Na2
HP1
Na1
TM7a
In
Solvent
Boudker O, et al, Nature 445:387(2007)

Figure S9